


© The Author(s), 2024. Published by Cambridge University Press on behalf of University of Arizona. This is an Open Access article, distributed under the terms of the Creative Commons Attribution licence (<http://creativecommons.org/licenses/by/4.0/>), which permits unrestricted re-use, distribution and reproduction, provided the original article is properly cited.

A VIEW FROM THE COUNTRYSIDE: RADIOCARBON CHRONOLOGY FOR ZAOLINHETAN OF THE PRE-ZHOU CULTURE IN EARLY DYNASTIC CHINA

Xiaojian Li¹ • Wei Liu¹ • Yongxiang Xu² • Haifeng Dou^{1*} • A Mark Pollard³ • Ruiliang Liu^{4*} 

¹Key Laboratory of Cultural Heritage Research and Conservation, School of Cultural Heritage, Northwest University China

²Ministry of Education Key Laboratory of Western China's Environmental Systems, College of Earth and Environmental Sciences, Lanzhou University, Lanzhou, China

³School of Archaeology, University of Oxford, Oxford, UK

⁴Department of Asia, British Museum, London, UK

ABSTRACT. The conquest of the Shang Dynasty at Anyang around 1046 BCE by the Zhou is one of the major events for not only Chinese Bronze Age but also early interaction between the pastoralist groups from the Eurasian Steppes and agriculture ones in the Central Plains of China. It is well-known from historical texts that the pre-Zhou people lived in the ancient Bin region (邠), the exact location of which is unclear, but most likely in the Jing River valley. At some point the leader Gugong Danfu (古公亶父) moved from Bin to the capital Qi (Zhouyuan), which preceded the Zhou invasion of Anyang. We have produced a new high resolution radiocarbon chronology for Zaolinheta, a small settlement in the pre-Zhou heartland. This shows not only an exceptionally long chronological span for the site, but also a different phasing compared to the traditional pottery typology, which raises new questions regarding the regional variation of pottery typologies. Intriguingly, the analysis also reveals a rapid abandonment of Zaolinheta around 1100 BCE, at the same time many larger sites, such as Zhouyuan, which later became the capital of the Western Zhou dynasty, were significantly expanding. We argue that the drastic decline of Zaolinheta as revealed by the substantial number of radiocarbon dates and probably also the movement of pre-Zhou political center from Bin to Qin, was part of bigger picture that involved a range of social and environmental factors.

KEYWORDS: early Dynastic China, Pre-Zhou Culture, radiocarbon dating, Shang, typo-chronology, western Zhou.

INTRODUCTION

Radiocarbon-based chronologies have become increasingly important in our understanding of early Dynastic China (Chen 2023; Liu 2020; XSZ Project 2022). A major step-change in this process was the development of Bayesian modeling which allowed radiocarbon dates from specified contexts to constrain the chronologies (Bayliss 2009; Bronk Ramsey 2019), leading to greater precision in the calibrated dates. Traditionally, Chinese archaeology has been built around stratigraphy and pottery typology, usually via the construction of a “master pottery sequence” using materials from major sites, such as early dynastic capitals (Zhang 1983; Yu 1996; Lin 2019). Whilst this has been spectacularly successful, it runs the danger of “normalizing” pottery sequences across large regions, thereby masking regional variations within such typologies. Specifically, it has the effect of projecting the typologies and associated chronologies seen in the major urban centers into smaller regional settlements. This paper investigates this phenomenon in the context of the pre-Zhou culture along the Jing River in present-day Shaanxi Province, China.

This project has focussed a large number of radiocarbon dates (n=101) on the relatively small-scale settlement of Zaolinheta located by the Jing River in Shaanxi Province (Figure 1). Although small compared to the major contemporary sites (e.g., Zhouyuan or Xitou), it is located in the heartland of the pre-Zhou culture in the Guanzhong region, which later moved eastwards and replaced the powerful Shang dynasty in the Central Plains to become the Zhou

*Corresponding authors. Emails: douhaifeng456@163.com; rliu@britishmuseum.org



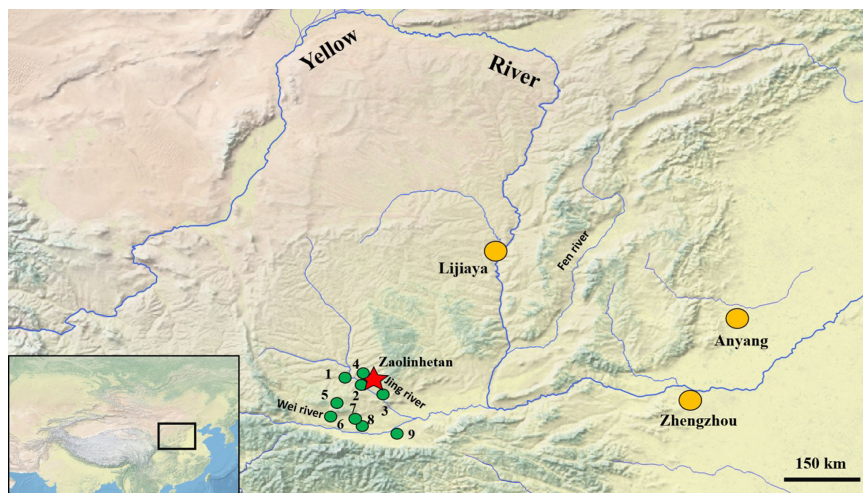


Figure 1 Geographic locations of the sites mentioned in the manuscript. Adjacent sites to Zaolinhetan: 1. Nianzipo, 2. Duanjing, 3. Zaoshugounao, 4. Xitou, 5. Caijiahe, 6. Zhouyuan, 7. Andi, 8. Zhengjiapo, 9. Feng-Hao.

dynasty, eventually expanding the Zhou territory from northwest China to the Yangtze River (Rawson 1999; Jaffe 2020). A substantial volume of literature has been centered on the chronology and motivations of this process, the earliest dynastic transition recorded in bronze inscriptions and historical documents (Grundmann 2019; Li 2018:28–37). The intensive radiocarbon study of the small-scale settlement Zaolinhetan reported here enables the finer chronology of this transition to be studied from the perspective of the pre-Zhou heartland. Since this is the first comprehensive radiocarbon dating project focused on the small-scale sites in this region, our sampling strategy attempts to set up a model practice that includes the whole sequence of the stratigraphy and provide suitable dating materials throughout the excavation, which should be of greater interests to archaeologists who hope for high-quality chronology in order to disentangle the development of the Zhou people and the conquest to the east.

MATERIALS AND METHODS

Zaolinhetan is located 13 km southwest of the present-day Zaolinhetan village of Xunyi county in Shaanxi province. It is essentially a small northeast-southwest loess mound surrounded by the Sanshui river along its northern, western and southern sides. Excavation was carried out by Northwest University China in 2016. The total area of the site is approximately 80,000 m². So far 1060 m² have been fully excavated, including 114 trash pits/hoards, three houses, 12 trash trenches and four tombs. The largest category of recovered objects is pottery, followed by stones, bones and bronzes. The *Li* vessel accounts for the majority of the pottery category. *Li* with divided or jointed crotch have been discovered at Zaolinhetan, which are the two classical pottery forms that have been widely associated with different group identities in the literature (Liu 2003; Zhang 2004; Lei 2010). The zooarchaeological studies reveal a variety of animal species, including pigs, dogs, sheep, goats, horses, cattle and many wild ones, suggesting a mixed economy with both agriculture and pastoralist practices (Li et al. 2019). This has been complemented by an archaeobotanical

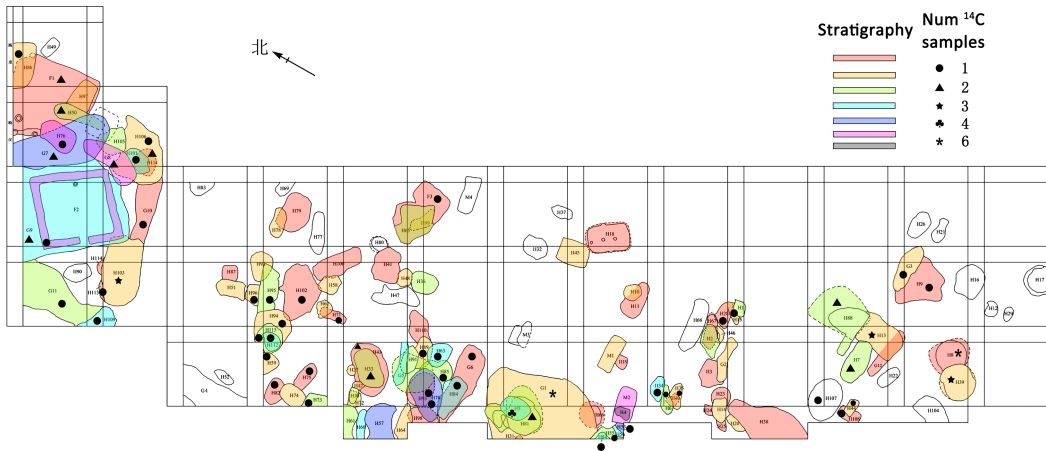


Figure 2 Floorplan of Zaolinhetao (the color of each strata merely indicates the relative sequence in the same archaeological group. Layers in the same color across different archaeological remains [e.g., different houses] do not necessarily suggest the same time).

study and stable isotopic analysis, demonstrating millet as staple for this region, followed by barley and soybeans (Chen et al. 2019).

Sampling Strategy

The objective is to create an overarching radiocarbon-based chronology for the entire site. The first step is to summarize the complex stratigraphic sequence (Figures 2 and 3). The most complex sequence was found in the northwest part of the site, involving six layers between the two largest houses (oldest F1 and youngest F2). In order to present the complete chronological sequence, 24 sequences have been selected in the next step, all of which contain two or more layers, with each one yielding at least one well-preserved sample for radiocarbon dating. Short-lived plant seeds are the most preferential dating materials due to their relatively simple carbon reservoirs, followed by human or animal bones.

Sample Pretreatment

Laboratory analyses were performed at the Oxford Radiocarbon Accelerator Unit in the Research Laboratory of Archaeology and the History of Art (RLAHA), University of Oxford. An additional 12 radiocarbon dates were obtained from Beta-laboratory during the excavation process for interlaboratory comparison. The full detailed pretreatment process can be found in Brock (2010). Calibration and Bayesian modeling was performed with IntCal 20 (Reimer et al. 2020) and OxCal (Bronk Ramsey 2021, version 4.4.4). Briefly, for the category of bone samples, the routine pretreatment procedure in RLAHA (coded AF) involves a simple ABA treatment that is commonly carried out in many other radiocarbon laboratories, followed by gelatinization and ultrafiltration. Samples are sequentially treated with 0.5M hydrochloric acid (3 or 4 rinses over ~18 hr), 0.1M sodium hydroxide (30 min), and 0.5M hydrochloric acid (1 hr) with thorough rinsing with ultrapure water between each reagent. The plant samples follow the similar sequential ABA pretreatment consisting of an initial hydrochloric acid wash (1M) for until effervescence has disappeared, then a sodium hydroxide base wash (0.2M) for 20 min and again 1M hydrochloric acid wash (80°C, coded VV).

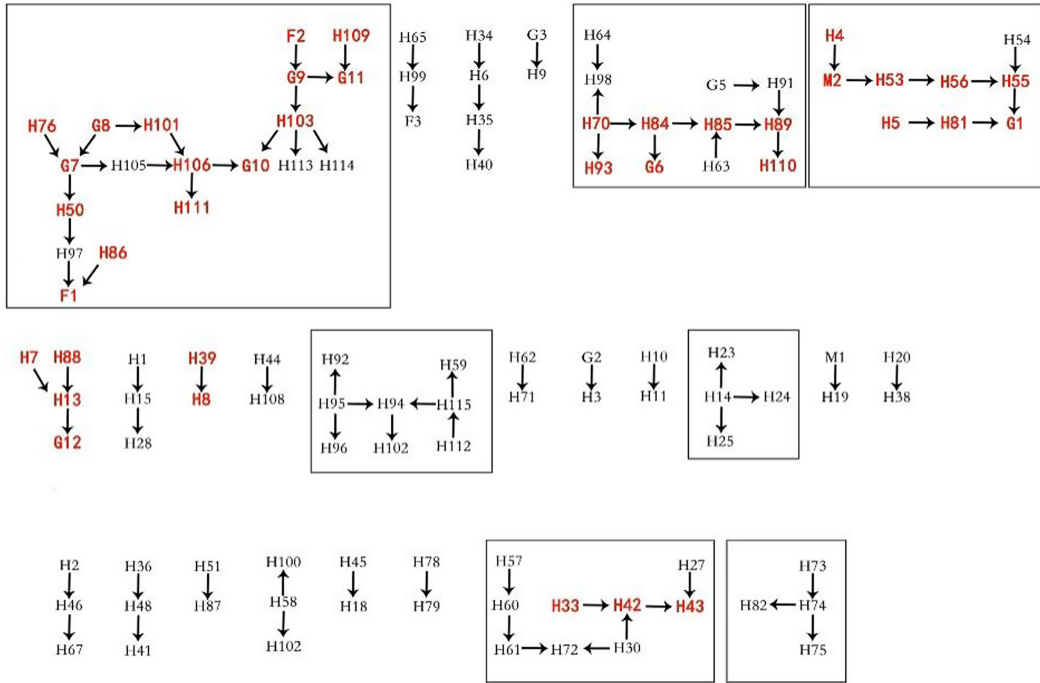


Figure 3 The matrix of stratigraphy in Zaolinhetan (arrow indicates that the upper layer [younger] breaks through the lower layer [older]. Archaeological units in red contain both abundant pottery for typological analysis and samples that were radiocarbon dated). (Please see online version for color figures.)

Bayesian Modeling

The main model structure follows a mainstream Sequence-Boundary-Phase structure (Bronk Ramsey 1998). The sequence of dates is determined by the excavation layer sequence (from old to young). Multiple samples are put in the same Phase if they were taken from the same excavation layer. Given that some samples are so small (e.g., plant seeds) that their positions are likely to be disturbed during deposition or excavation, we apply an Outlier model in order to identify samples that were mislocated. The model parameters are default as (student t distribution, freedom 5, uncertainty $10^0 \sim 10^4$ and t-type outlier) and each sample is set with 0.05 prior probability to be an outlier (Bronk Ramsey 2009).

RESULTS AND DISCUSSION

New Chronological Phasing

All the results can be found in Table 1. The Bayesian Outlier model was applied to reconstruction of the whole chronology. It also helps to examine the consistency between the radiocarbon results and the stratigraphic sequence. The two types of chronological information show good agreement, with only a few exceptions (Beta 15/16, XD-66/18/56) to be outlier based on their high posterior outlier probability (Bronk Ramsey 2009). The samples Beta-15 and 16 appear much younger compared to their excavation layers so very likely to be later samples falling into the older layers. Opposite cases can be found in XD-66/18/56, of which the radiocarbon dates are much older compared to other samples in the same stratigraphy. The

Table 1 Radiocarbon results for Zaolinhetan (The excavation numbers contain information on the year and the unit/cultural layer of the excavation unit. The sample number is assigned by the excavators when selecting samples for radiocarbon dating. The lab numbers are assigned by the radiocarbon laboratories).

Archaeological unit	Excavation number	Sample material	Sample number	Lab number	Radiocarbon results	$\delta^{13}\text{C}$	Calibrated date (95.4%)	Calibrated date (68.3%)
F1	2016XZA F1③	Animal bone	XD-4	OxA-42265	2959 ± 21	-17.48	(93.4%)1261–1110 cal BCE (1.1%)1093–1083 cal BCE	(25.3%)1216–1187 cal BCE (22.5%)1181–1155 cal BCE
F1	FX2 F1①-1	Millet	XD-59	OxA-X-3131-16	3227 ± 35	-10.15	(1.0%)1066–1058 cal BCE (2.3%)1602–1584 cal BCE	(20.5%)1149–1126 cal BCE (68.3%)1516–1447 cal BCE
F2	2016XZA F2	Animal bone	XD-3	OxA-41778	2909 ± 25	-8.13	(73.2%)1134–1013 cal BCE (22.3%)1203–1141 cal BCE	(2.7%)1187–1181 cal BCE (3.9%)1156–1148 cal BCE (59.8%)1127–1047 cal BCE (1.9%)1027–1023 cal BCE
F3	FX21 F3-1	Millet	XD-58	OxA-41385	2915 ± 19	-8.98	(64.5%)1134–1042 cal BCE (26.3%)1206–1140 cal BCE (4.7%)1035–1017 cal BCE	(3.7%)1187–1181 cal BCE (5.3%)1156–1148 cal BCE (59.3%)1127–1052 cal BCE
G1	2016XZA G1①	Animal bone	XD-12	OxA-41373	2943 ± 20	-15.09	(95.4%)1220–1054 cal BCE	(68.3%)1204–1121 cal BCE
G1	FX15 G1①-1	Millet	XD-56	OxA-X-3131-15	3291 ± 49	-10.20	(89.1%) 1687–1490 cal BCE (6.4%) 1484–1449 cal BCE	(68.3%)1614–1508 cal BCE
G1	FX18 G1①-2	Millet	XD-57	OxA-41496	2972 ± 23	-9.26	(95.4%)1277–1113 cal BCE	(5.7%)1256–1247 cal BCE (30.9%)1227–1189 cal BCE (16.4%)1179–1157 cal BCE (15.3%)1146–1128 cal BCE
G1	2016XZA G1③	Animal bone	XD-11	OxA-41372	2950 ± 20	-6.82	(94.3%)1226–1055 cal BCE (1.1%)1255–1248 cal BCE	(68.3%)1206–1119 cal BCE
G1	2016XZA G1⑥	Animal bone	XD-10	OxA-41371	2941 ± 20	-19.83	(95.4%)1218–1055 cal BCE	(68.3%)1206–1119 cal BCE
G3	2016XZA G3	Animal bone	XD-8	OxA-X-3122-30	2962 ± 25	-16.56	(91.7%)1265–1108 cal BCE (2.0%)1096–1080 cal BCE (1.7%)1069–1056 cal BCE	(68.3%)1219–1126 cal BCE
G6	2016XZA G6	Animal bone	XD-13	OxA-41374	3000 ± 20	-6.83	(80.1%)1300–1189 cal BCE (5.3%)1182–1158 cal BCE (5.1%)1376–1352 cal BCE (5.0%)1146–1128 cal BCE	(68.3%)1277–1208 cal BCE
G7	2016XZA G7①	Animal bone	XD-1	OxA-41275	2958 ± 19	-6.71	(94.0%)1260–1111 cal BCE (0.8%)1092–1084 cal BCE (0.6%)1065–1059 cal BCE	(24.6%)1215–1187 cal BCE (22.8%)1181–1155 cal BCE (20.9%)1149–1126 cal BCE

(Continued)

Table 1 (Continued)

Archaeological unit	Excavation number	Sample material	Sample number	Lab number	Radiocarbon results	$\delta^{13}\text{C}$	Calibrated date (95.4%)	Calibrated date (68.3%)
G7	2016XZA G7①	Animal bone	XD-1 (repeated analysis)	OxA-41276	2963 ± 19	-6.81	(95.4%)1261–1115 cal BCE	(27.5%)1219–1187 cal BCE (21.1%)1181–1156 cal BCE (19.7%)1148–1127 cal BCE (68.3%)1202–1125 cal BCE
G7	2016XZA G7②	Animal bone	XD-2	OxA-41277	2949 ± 19	-13.42	(88.3%)1225–1106 cal BCE (3.8%)1099–1077 cal BCE (3.0%)1072–1055 cal BCE (0.4%)1253–1250 cal BCE	(6.9%)1257–1247 cal BCE (32.1%)1228–1192 cal BCE (14.4%)1177–1159 cal BCE (14.9%)1145–1128 cal BCE (10.5%)1259–1243 cal BCE (31.4%)1233–1191 cal BCE (13.4%)1178–1158 cal BCE (13.0%)1146–1128 cal BCE
G8	FX45 G8-1	Millet	XD-55	OxA-41495	2974 ± 20	-9.99	(95.4%)1266–1121 cal BCE	(6.9%)1257–1247 cal BCE (32.1%)1228–1192 cal BCE (14.4%)1177–1159 cal BCE (14.9%)1145–1128 cal BCE
G8	FX45 G8-1	Millet	XD-54	OxA-41544	2976 ± 25	-9.25	(94.8%)1286–1113 cal BCE (0.6%)1368–1359 cal BCE	(10.5%)1259–1243 cal BCE (31.4%)1233–1191 cal BCE (13.4%)1178–1158 cal BCE (13.0%)1146–1128 cal BCE
G9	2016XZA G9①	Animal bone	XD-7	OxA-X-3122-29	2957 ± 18	-13.98	(91.0%)1234–1111 cal BCE (3.0%)1259–1242 cal BCE (0.8%)1092–1084 cal BCE (0.6%)1065–1059 cal BCE	(24.1%)1214–1187 cal BCE (22.9%)1180–1155 cal BCE (21.3%)1149–1126 cal BCE
G9	2016XZA G9②	Animal bone	XD-6	OxA-41279	2986 ± 18	-11.90	(83.7%)1276–1154 cal BCE (11.8%)1149–1126 cal BCE	(62.2%)1261–1200 cal BCE (6.1%)1141–1133 cal BCE
G10	2016XZA G10	Animal bone	XD-5	OxA-41278	2959 ± 19	-19.10	(94.9%)1260–1112 cal BCE (0.3%)1088–1086 cal BCE (0.3%)1063–1060 cal BCE	(25.2%)1216–1187 cal BCE (22.4%)1181–1155 cal BCE (20.6%)1149–1126 cal BCE
G11	FX35 G11-1	Millet	XD-53	OxA-41543	3011 ± 24	-9.67	(76.5%)1310–1193 cal BCE (13.7%)1383–1342 cal BCE (2.7%)1144–1129 cal BCE (2.5%)1176–1160 cal BCE	(2.9%)1366–1361 cal BCE (65.3%)1288–1215 cal BCE
H5	FX29 H5-1	Millet	XD-71	OxA-41498	3027 ± 18	-10.14	(71.5%)1311–1216 cal BCE (24.0%)1384–1341 cal BCE	(13.4%)1372–1355 cal BCE (40.0%)1297–1257 cal BCE (14.8%)1246–1228 cal BCE
H5	FX29 H5-1	Millet	XD-70	OxA-41406	2900 ± 18	-9.56	(88.0%)1129–1012 cal BCE (4.2%)1193–1176 cal BCE (3.3%)1159–1146 cal BCE	(66.0%)1120–1047 cal BCE (2.2%)1027–1023 cal BCE
H5	FX52 H5-2	Millet	XD-69	OxA-X-3131-20	3320 ± 52	-10.12	(88.9%)1699–1497 cal BCE (5.5%)1741–1710 cal BCE (1.0%)1473–1461 cal BCE	(2.4%)1666–1659 cal BCE (65.9%)1632–1514 cal BCE

Table 1 (Continued)

Archaeological unit	Excavation number	Sample material	Sample number	Lab number	Radiocarbon results	$\delta^{13}\text{C}$	Calibrated date (95.4%)	Calibrated date (68.3%)
H5	FX52 H5-2	Millet	XD-68	OxA-41420	2960 ± 20	-8.97	(94.2%)1261–1111 cal BCE (0.7%)1091–1084 cal BCE (0.5%)1064–1059 cal BCE	(25.8%)1217–1187 cal BCE (22.1%)1181–1155 cal BCE (20.3%)1149–1126 cal BCE
H6	2016XZA H6	Animal bone	XD-34	OxA-41584	2950 ± 17	-12.48	(90.5%)1225–1107 cal BCE (2.4%)1096–1079 cal BCE (2.1%)1070–1055 cal BCE (0.5%)1253–1249 cal BCE	(60.3%)1205–1125 cal BCE
H7	FX46 H7-1	Millet	XD-67	OxA-41545	2862 ± 25	-10.67	(86.8%)1119–967 cal BCE (8.7%)961–931 cal BCE	(5.6%)1107–1096 cal BCE (6.3%)1081–1068 cal BCE (56.4%)1056–985 cal BCE
H7	FX46 H7-1	Millet	XD-66	OxA-X-3131-18	3177 ± 27	-9.95	(95.4%)1503–1412 cal BCE	(24.3%)1496–1476 cal BCE (44.0%)1458–1423 cal BCE
H8⊙	FX40 H8⊙-1	Soybean	XD-60	OxA-41386	2932 ± 19	-25.06	(95.4%)1214–1052 cal BCE	(48.0%)1202–1140 cal BCE (18.4%)1134–1110 cal BCE (1.9%)1063–1060 cal BCE
H8⊙	FX40 H8⊙-1	Millet	XD-61	OxA-41497	3003 ± 21	-9.57	(80.5%)1301–1192 cal BCE (6.9%)1377–1350 cal BCE (4.1%)1145–1129 cal BCE (4.0%)1178–1160 cal BCE	(68.3%)1281–1210 cal BCE
H8⊙	FX41 H8⊙-1	Millet	XD-65	OxA-41343	2950 ± 18	-9.40	(88.9%)1226–1106 cal BCE (3.2%)1099–1077 cal BCE (2.5%)1071–1055 cal BCE (0.8%)1255–1248 cal BCE	(68.3%)1205–1125 cal BCE
H8⊙	FX41 H8⊙-1	Millet	XD-65 (repeated analysis)	OxA-41344	2953 ± 17	-9.59	(91.3%)1228–1109 cal BCE (1.5%)1094–1082 cal BCE (1.4%)1256–1246 cal BCE (1.3%)1068–1057 cal BCE	(21.3%)1211–1186 cal BCE (47.0%)1180–1126 cal BCE
H8⊙	FX1 H8⊙-1	Millet	XD-63	OxA-X-3131-17	3069 ± 25	-10.53	(95.4%)1413–1263 cal BCE	(40.8%)1394–1334 cal BCE (27.4%)1325–1287 cal BCE
H8⊙	FX1 H8⊙-1	Millet	XD-62	OxA-41419	3259 ± 20	-8.77	(76.9%)1546–1493 cal BCE (9.9%)1481–1452 cal BCE (7.6%)1609–1577 cal BCE (1.1%)1561–1554 cal BCE	(68.3%)1536–1501 cal BCE
H9	2016XZA H9⊙	Animal bone	XD-35	OxA-41467	2961 ± 18	-18.19	(95.4%)1260–1115 cal BCE	(26.6%)1217–1188 cal BCE (21.3%)1180–1156 cal BCE (20.4%)1148–1127 cal BCE

(Continued)

Table 1 (Continued)

Archaeological unit	Excavation number	Sample material	Sample number	Lab number	Radiocarbon results	$\delta^{13}\text{C}$	Calibrated date (95.4%)	Calibrated date (68.3%)
H13⑥	FX47 H13⑥-1	Soybean	XD-86	OxA-41549	3016 ± 43	-26.94	(95.4%)1399–1124 cal BCE	(15.7%)1381–1344 cal BCE (52.6%)1307–1206 cal BCE
H13⑥	FX47 H13⑥-1	Millet	XD-87	OxA-42243	3008 ± 35	-9.01	(80.2%)1318–1125 cal BCE (15.3%)1387–1338 cal BCE	(9.1%)1374–1352 cal BCE (57.8%)1300–1202 cal BCE (1.4%)1139–1135 cal BCE
H13⑥	FX50 H13⑥-1	Millet	XD-88	OxA-41586	2960 ± 17	-9.54	(91.6%)1236–1114 cal BCE (3.8%)1260–1241 cal BCE	(25.8%)1216–1188 cal BCE (21.8%)1180–1156 cal BCE (20.6%)1148–1127 cal BCE
H15	2016XZA H15	Sheep/goat	XD-36	OxA-41474	2966 ± 18	-14.25	(95.4%)1260–1120 cal BCE	(29.3%)1221–1187 cal BCE (20.0%)1181–1156 cal BCE (19.0%)1148–1127 cal BCE
H28	2016XZA H28	Animal bone	XD-37	OxA-41475	3028 ± 17	-16.31	(71.0%)1311–1217 cal BCE (24.5%)1384–1341 cal BCE	(14.3%)1372–1355 cal BCE (41.7%)1297–1258 cal BCE (12.3%)1245–1230 cal BCE
H33 H33	2016XZA H33 FX6 H33-1	Sheep/goat Millet	XD-38 XD-84	OxA-41476 OxA-41547	2935 ± 17 3040 ± 36	-18.62 -9.20	(95.4%)1213–1055 cal BCE (95.4%)1412–1202 cal BCE	(68.3%)1205–1113 cal BCE (26.0%)1384–1341 cal BCE (34.9%)1313–1258 cal BCE (7.4%)1245–1230 cal BCE
H34	2016XZA H34	Animal bone	XD-39	OxA-41477	2960 ± 17	-14.40	(91.6%)1236–1114 cal BCE (3.8%)1260–1241 cal BCE	(25.8%)1216–1188 cal BCE (21.8%)1180–1156 cal BCE (20.6%)1148–1127 cal BCE
H34	2016XZA H34	Animal bone	XD-39 (repeated analysis)	OxA-41478	2980 ± 17	-14.52	(95.4%)1265–1125 cal BCE	(13.6%)1258–1243 cal BCE (36.0%)1232–1197 cal BCE (7.9%)1173–1163 cal BCE
H35	FX17 H35-1	Millet	XD-83	OxA-41585	2952 ± 17	-9.17	(91.1%)1227–1109 cal BCE (1.8%)1095–1081 cal BCE (1.6%)1068–1056 cal BCE (1.0%)1255–1247 cal BCE	(20.0%)1208–1186 cal BCE (10.9%)1143–1131 cal BCE (48.3%)1180–1126 cal BCE
H39	2016XZA H39⑥	Animal bone	XD-40	OxA-41479	2970 ± 18	-15.40	(95.4%)1261–1122 cal BCE	(32.3%)1224–1189 cal BCE (18.4%)1179–1157 cal BCE (17.6%)1146–1128 cal BCE
H39	2016XZA H39⑥	Animal bone	XD-41	OxA-41480	2944 ± 17	-11.03	(87.2%)1220–1106 cal BCE (4.6%)1099–1077 cal BCE (3.6%)1071–1055 cal BCE	(68.3%)1204–1122 cal BCE

Table 1 (Continued)

Archaeological unit	Excavation number	Sample material	Sample number	Lab number	Radiocarbon results	$\delta^{13}\text{C}$	Calibrated date (95.4%)	Calibrated date (68.3%)
H39	2016XZA H39 [Ⓢ]	Animal bone	XD-42	OxA-41481	2963 ± 17	-10.75	(95.4%)1260–1117 cal BCE	(27.6%)1218–1188 cal BCE (20.8%)1180–1157 cal BCE (19.8%)1147–1127 cal BCE
H43	FX7 H43-1	Millet	XD-82	OxA-X-3131-31	3066 ± 29	-10.27	(93.5%)1415–1259 cal BCE (1.9%)1243–1232 cal BCE	(40.0%)1391–1335 cal BCE (28.3%)1323–1284 cal BCE
H43	FX7 H43-1	Millet	XD-81	OxA-41546	3032 ± 29	-10.04	(95.4%)1400–1204 cal BCE	(20.0%)1378–1347 cal BCE (35.5%)1304–1256 cal BCE (12.8%)1248–1226 cal BCE
H44	2016XZA H44	Animal bone	XD-43	OxA-41482	2945 ± 17	-12.90	(87.8%)1221–1106 cal BCE (4.3%)1099–1077 cal BCE (3.3%)1071–1055 cal BCE	(68.3%)1203–1123 cal BCE
H50	FX28 H50-1	Millet	XD-80	OxA-41348	3020 ± 19	-9.26	(77.0%)1311–1206 cal BCE (18.4%)1384–1341 cal BCE	(4.5%)1367–1360 cal BCE (63.8%)1290–1223 cal BCE
H50	FX28 H50-1	Millet	XD-79	OxA-41347	2994 ± 18	-9.26	(86.7%)1290–1157 cal BCE (7.0%)1146–1127 cal BCE (1.8%)1370–1358 cal BCE	(68.3%)1266–1203 cal BCE
H53	2016XZA H53	Animal bone	XD-44	OxA-41334	2962 ± 17	-19.00	(95.4%)1260–1116 cal BCE	(27.1%)1218–1189 cal BCE (20.9%)1179–1157 cal BCE (20.2%)1147–1127 cal BCE
H54	2016XZA H54	Animal bone	XD-24	OxA-41400	2940 ± 19	-6.45	(95.4%)1217–1055 cal BCE	(68.3%)1206–1118 cal BCE
H55	2016XZA H55	Animal bone	XD-25	OxA-41401	2934 ± 19	-17.34	(95.4%)1214–1053 cal BCE	(68.3%)1206–1111 cal BCE
H59	2016XZA H59	Animal bone	XD-26	OxA-41402	2961 ± 18	-15.25	(95.4%)1260–1115 cal BCE	(26.6%)1217–1188 cal BCE (21.3%)1180–1156 cal BCE (20.4%)1148–1127 cal BCE
H63	2016XZA H63	Animal bone	XD-27	OxA-41463	2969 ± 18	-7.40	(95.4%)1261–1122 cal BCE	(31.5%)1224–1188 cal BCE (18.8%)1180–1157 cal BCE (18.0%)1147–1127 cal BCE
H70	2016XZA H70	Animal bone	XD-28	OxA-41403	2988 ± 19	-7.28	(95.4%)1282–1125 cal BCE	(63.0%)1263–1200 cal BCE (5.3%)1141–1133 cal BCE
H71	2016XZA H71	Animal bone	XD-29	OxA-41404	2964 ± 19	-19.77	(95.4%)1261–1116 cal BCE	(28.1%)1220–1187 cal BCE (20.7%)1181–1156 cal BCE (19.4%)1148–1127 cal BCE
H73	2016XZA H73	Animal bone	XD-30	OxA-41405	2961 ± 19	-14.09	(95.4%)1261–1112 cal BCE	(26.7%)1218–1187 cal BCE (21.4%)1180–1156 cal BCE (20.2%)1148–1127 cal BCE

(Continued)

Table 1 (Continued)

Archaeological unit	Excavation number	Sample material	Sample number	Lab number	Radiocarbon results	$\delta^{13}\text{C}$	Calibrated date (95.4%)	Calibrated date (68.3%)
H75	2016XZA H75	Animal bone	XD-31	OxA-41464	2988 ± 18	-16.11	(84.9%)1280–1154 cal BCE (10.5%)1149–1126 cal BCE	(63.7%)1262–1200 cal BCE (4.6%)1140–1134 cal BCE
H76	FX23 H76③-1	Millet	XD-85	OxA-41548	3002 ± 28	-10.32	(79.4%)1305–1155 cal BCE (9.5%)1380–1345 cal BCE (6.6%)1149–1126 cal BCE	(1.6%)1365–1361 cal BCE (64.4%)1287–1201 cal BCE (2.3%)1140–1134 cal BCE
H81	FX34 H81-5	Millet	XD-78	OxA-41346	2953 ± 18	-9.64	(90.5%)1229–1109 cal BCE (1.7%)1094–1081 cal BCE (1.6%)1257–1246 cal BCE (1.6%)1068–1056 cal BCE	(21.6%)1211–1186 cal BCE (46.7%)1180–1126 cal BCE
H82	2016XZA H82	Animal bone	XD-32	OxA-41465	2982 ± 18	-12.44	(95.4%)1268–1125 cal BCE	(16.5%)1260–1241 cal BCE (36.3%)1235–1197 cal BCE (6.1%)1172–1164 cal BCE
H84	2016XZA H84	Animal bone	XD-33	OxA-41466	2927 ± 18	-16.06	(95.4%)1211–1050 cal BCE	(9.4%)1143–1131 cal BCE (17.3%)1197–1172 cal BCE (15.7%)1163–1143 cal BCE (18.2%)1131–1107 cal BCE (9.2%)1096–1080 cal BCE (7.9%)1069–1056 cal BCE
H85	2016XZA H85	Animal bone	XD-45	OxA-41335	2941 ± 17	-16.91	(84.9%)1218–1105 cal BCE (10.5%)1100–1055 cal BCE	(68.3%)1202–1120 cal BCE
H86	2016XZA H86	Animal bone	XD-46	OxA-41336	2950 ± 17	-16.14	(90.5%)1225–1107 cal BCE (2.4%)1096–1079 cal BCE (2.1%)1070–1055 cal BCE (0.5%)1253–1249 cal BCE	(68.3%)1205–1125 cal BCE
H88	FX49 H88①-1	Millet	XD-75	OxA-41423	2955 ± 20	-9.29	(89.0%)1233–1109 cal BCE (1.8%)1095–1081 cal BCE (1.6%)1068–1056 cal BCE (3.0%)1259–1243 cal BCE	(22.8%)1213–1186 cal BCE (45.5%)1180–1126 cal BCE
H88	FX49 H88①-1	Millet	XD-76	OxA-41345	2945 ± 18	-9.69	(95.4%)1221–1055 cal BCE	(68.3%)1203–1123 cal BCE
H89	2016XZA H89	Animal bone	XD-47	OxA-41743	2963 ± 19	-12.25	(95.4%)1261–1115 cal BCE	(27.5%)1219–1187 cal BCE (21.1%)1181–1156 cal BCE (19.7%)1148–1127 cal BCE
H93	2016XZA H93	Animal bone	XD-48	OxA-41337	2970 ± 17	-18.01	(95.4%)1260–1123 cal BCE	(32.3%)1224–1190 cal BCE (18.1%)1179–1158 cal BCE (17.8%)1146–1128 cal BCE

Table 1 (Continued)

Archaeological unit	Excavation number	Sample material	Sample number	Lab number	Radiocarbon results	$\delta^{13}\text{C}$	Calibrated date (95.4%)	Calibrated date (68.3%)
H94	2016XZA H94	Animal bone	XD-49	OxA-41338	3000 ± 17	-16.16	(84.5%)1295–1193 cal BCE (3.8%)1144–1129 cal BCE (3.6%)1176–1160 cal BCE (3.5%)1372–1355 cal BCE	(68.3%)1271–1211 cal BCE
H95	2016XZA H95	Animal bone	XD-50	OxA-41339	2987 ± 17	-15.54	(84.7%)1276–1156 cal BCE (10.7%)1148–1126 cal BCE	(63.5%)1261–1201 cal BCE (4.8%)1140–1134 cal BCE
H96	2016XZA H96	Animal bone	XD-51	OxA-41340	2988 ± 17	-15.09	(85.3%)1278–1156 cal BCE (10.2%)1148–1126 cal BCE	(64.4%)1262–1201 cal BCE (3.9%)1140–1134 cal BCE
H101	FX44 H101-1	Soybean	XD-74	OxA-41422	2974 ± 20	-24.44	(95.4%)1266–1121 cal BCE	(6.9%)1257–1247 cal BCE (32.1%)1228–1192 cal BCE (14.4%)1177–1159 cal BCE (14.9%)1145–1128 cal BCE
H102	2016XZA H102	Animal bone	XD-52	OxA-41341	3005 ± 17	-15.55	(85.3%)1300–1195 cal BCE (6.1%)1376–1352 cal BCE (2.1%)1143–1131 cal BCE (1.9%)1174–1163 cal BCE	(68.3%)1271–1216 cal BCE
H103	2016XZA H103⊙	Animal bone	XD-14	OxA-41375	2919 ± 20	-16.77	(92.5%)1209–1045 cal BCE (3.0%)1031–1019 cal BCE	(5.8%)1189–1180 cal BCE (7.7%)1157–1146 cal BCE (54.8%)1128–1054 cal BCE
H103	2016XZA H103⊙	Animal bone	XD-15	OxA-41376	2977 ± 20	-15.50	(95.4%)1267–1122 cal BCE	(10.5%)1258–1244 cal BCE (33.2%)1231–1194 cal BCE (11.7%)1176–1160 cal BCE (12.9%)1144–1129 cal BCE
H103	2016XZA H103⊙	Animal bone	XD-16	OxA-41377	2970 ± 20	-7.39	(95.4%)1263–1121 cal BCE	(2.6%)1254–1249 cal BCE (30.9%)1225–1188 cal BCE (17.8%)1180–1157 cal BCE (16.9%)1147–1127 cal BCE
H106	2016XZA H106	Animal bone	XD-17	OxA-41378	2974 ± 22	-15.08	(95.4%)1273–1117 cal BCE	(7.7%)1257–1246 cal BCE (31.5%)1229–1191 cal BCE (14.5%)1178–1158 cal BCE (14.6%)1146–1128 cal BCE
H107	2016XZA H107	Animal bone	XD-18	OxA-41379	4017 ± 23	-6.29	(95.4%)2578–2470 cal BCE	(16.5%)2572–2556 cal BCE (31.9%)2543–2514 cal BCE (14.9%)2502–2488 cal BCE (5.1%)2482–2476 cal BCE

(Continued)

Table 1 (Continued)

Archaeological unit	Excavation number	Sample material	Sample number	Lab number	Radiocarbon results	$\delta^{13}\text{C}$	Calibrated date (95.4%)	Calibrated date (68.3%)
H108	2016XZA H108	Animal bone	XD-19	OxA-41380	3022 ± 20	-14.39	(74.9%)1314–1208 cal BCE (20.5%)1385–1340 cal BCE	(7.0%)1368–1358 cal BCE (61.3%)1293–1224 cal BCE
H108	2016XZA H108	Animal bone	XD-19 (repeated analysis)	OxA-41381	3019 ± 21	-14.30	(76.9%)1313–1200 cal BCE (18.6%)1385–1340 cal BCE	(5.0%)1367–1360 cal BCE (63.3%)1290–1221 cal BCE
H109	2016XZA H109	Animal bone	XD-20	OxA-41382	2969 ± 21	-16.75	(95.4%)1266–1116 cal BCE	(31.2%)1225–1187 cal BCE (19.1%)1181–1156 cal BCE (18.0%)1148–1127 cal BCE
H111	FX43 H111-1	Millet	XD-72	OxA-41421	3022 ± 21	-9.06	(74.5%)1316–1204 cal BCE (20.9%)1386–1339 cal BCE	(7.9%)1369–1357 cal BCE (60.4%)1294–1224 cal BCE
H111	FX43 H111-1	Millet	XD-73	OxA-41773	2980 ± 40	-8.37	(90.3%)1304–1054 cal BCE (5.1%)1379–1347 cal BCE	(56.8%)1264–1155 cal BCE (11.5%)1149–1126 cal BCE
H112	2016XZA H112	Animal bone	XD-21	OxA-41383	2991 ± 20	-13.21	(84.9%)1286–1155 cal BCE (9.4%)1149–1126 cal BCE (1.1%)1367–1360 cal BCE	(63.8%)1265–1200 cal BCE (4.5%)1141–1133 cal BCE
H113	2016XZA H113	Animal bone	XD-22	OxA-41384	3010 ± 20	-6.74	(81.2%)1305–1196 cal BCE (11.0%)1380–1346 cal BCE (1.7%)1143–1132 cal BCE (1.5%)1174–1163 cal BCE	(68.3%)1284–1216 cal BCE
H115	2016XZA H115	Animal bone	XD-23	OxA-41399	2960 ± 19	-18.22	(95.4%)1261–1112 cal BCE	(26.0%)1217–1187 cal BCE (21.8%)1180–1156 cal BCE (20.4%)1148–1127 cal BCE
M1	2016XZAM1	Fibula (human)	Beta-1	Beta-447594	2760 ± 30	-7.7	(95.4%)990~826 cal BCE	(32.0%)930–891 cal BCE (36.3%)882–1835 cal BCE
M3	2016XZAM3	Skeletal (human)	Beta-2	Beta-447595	2770 ± 30	-7.8	(95.4%)999~832 cal BCE	(11.7%)973–955 cal BCE (34.0%)933–896 cal BCE (22.6%)873–840 cal BCE
H88	2016XZAH88 [Ⓢ]	Mandibular bone (dog)	Beta-3	Beta-447596	2900 ± 30	-7.8	(95.4%)1209~1005 cal BCE	(68.3%)1124–1016 cal BCE
F3	2016XZAF3	Mandibular bone (dog)	Beta-4	Beta-447597	2860 ± 30	-7	(95.4%)1122~927 cal BCE	(5.4%)1107–1096 cal BCE (6.1%)1081–1068 cal BCE (53.2%)1056–981 cal BCE (3.7%)947–939 cal BCE
H8	2016XZAH8 [Ⓢ]	Limb bone (cow or horse)	Beta-5	Beta-447598	2880 ± 30	-12.6	(3.5%)1197~1173 cal BCE (2.8%)1162~1143 cal BCE (85.8%)1130~973 cal BCE (3.3%)956~933 cal BCE	(68.3%)1112–1012 cal BCE
H99	2016XZAH99	Palatinate (sheep)	Beta-6	Beta-447599	2850 ± 30	-15	(95.4%)1114~924 cal BCE	(55.5%)1053–972 cal BCE (12.7%)956–933 cal BCE

Table 1 (Continued)

Archaeological unit	Excavation number	Sample material	Sample number	Lab number	Radiocarbon results	$\delta^{13}\text{C}$	Calibrated date (95.4%)	Calibrated date (68.3%)
H91	2016XZAH91	Radial bone (cow)	Beta-7	Beta-447600	2900 ± 30	-15.3	(95.4%)1209~1005 cal BCE	(68.3%)1124–1016 cal BCE
M2	2016XZAM2	Metatarsal bone (human)	Beta-8	Beta-544094	2930 ± 30	-6.8	(95.4%)1222~1016 cal BCE	(37.0%)1201–1140 cal BCE (16.5%)1134–1107 cal BCE (8.1%)1096–1080 cal BCE (6.7%)1069–1056 cal BCE
H45	2016A2 H45③: CN4	Animal bone	Beta-9	Beta-544095	2940 ± 30	-15.2	(1.9%)1258~1245 cal BCE (92.2%)1230~1046 cal BCE (1.3%)1030~1020 cal BCE	(67.2%)1215–1110 cal BCE (1.1%)1063–1060 cal BCE
H65	2016A3 H65: CN3	Animal bone	Beta-10	Beta-544096	2940 ± 30	-11.1	(1.9%)1258~1245 cal BCE (92.2%)1230~1046 cal BCE (1.3%)1030~1020 cal BCE	(67.2%)1215–1110 cal BCE (1.1%)1063–1060 cal BCE
H81	2016A4 H81: CN1	Animal bone	Beta-11	Beta-544097	3210 ± 30	-16.6	(95.4%)1519~1422 cal BCE	(68.3%)1503–1447 cal BCE
H103	2016A5 H103③: CN5	Animal bone	Beta-12	Beta-544098	2900 ± 30	-14.8	(95.4%)1209~1005 cal BCE	(68.3%)1124–1016 cal BCE

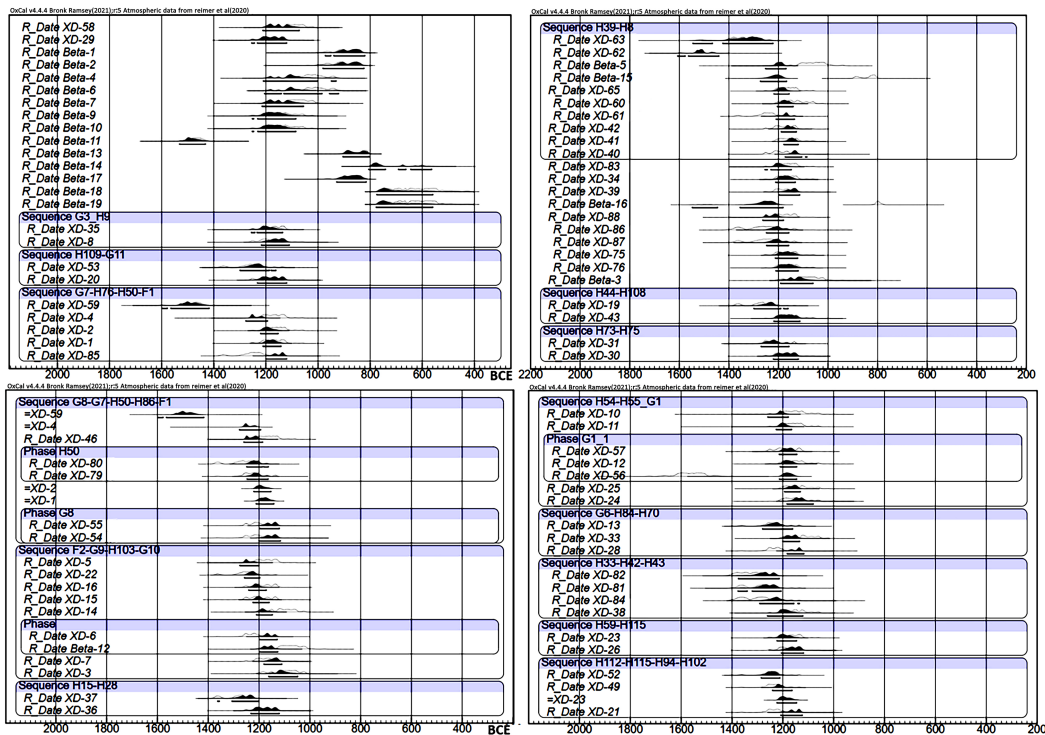


Figure 4 Bayesian modeled chronology of Zaolinhetan (Sequence_Boundary_Phase models built in the Outlier Model).

majority of the radiocarbon dates ($n = 96$) are well consistent with the excavation sequence. It is worth of pointing out that the radiocarbon experts were involved in the very beginning of the excavation, therefore the importance of the small plant materials and animal, together with their relative excavation sequence, was repeatedly discussed throughout excavation.

Methods for summarizing a large set of radiocarbon data have been extensively discussed in the literature (see reference in Bronk Ramsey 2017). Whilst the Sum function, essentially to stack the dates and uncertainties together, has been widely applied to radiocarbon dates, there are a few issues with this method because of the noise due to the limited number of dated samples, noise from the calibration process, and excessive spread due to measurement uncertainty (Bronk Ramsey 2017). The current study adopts the most recently developed method of the kernel density estimate (KDE). Following the widely used normal kernel and optimal bandwidth, KDE helps to overcome these issues and better visualize the relatively large number of radiocarbon data here (Bronk Ramsey 2017). OxCal provides convenient tools for KDE analysis. Here the default command is employed, using the normal kernel $\sim N(0,1)$ and the factor according to Silverman’s rule ($\sim U(0,1)$). It is important to note that although KDE is a frequentist approach, similar to Sum, it can be built in a radiocarbon Bayesian model and take advantage of the posterior data.

As illustrated in Figure 5, the radiocarbon results illustrate a continuous occupation at Zaolinhetan since the 16th century BCE, but its major occupation appears well-correlated with a number of the key periods of the Shang dynasty (Figure 4). The earliest radiocarbon date

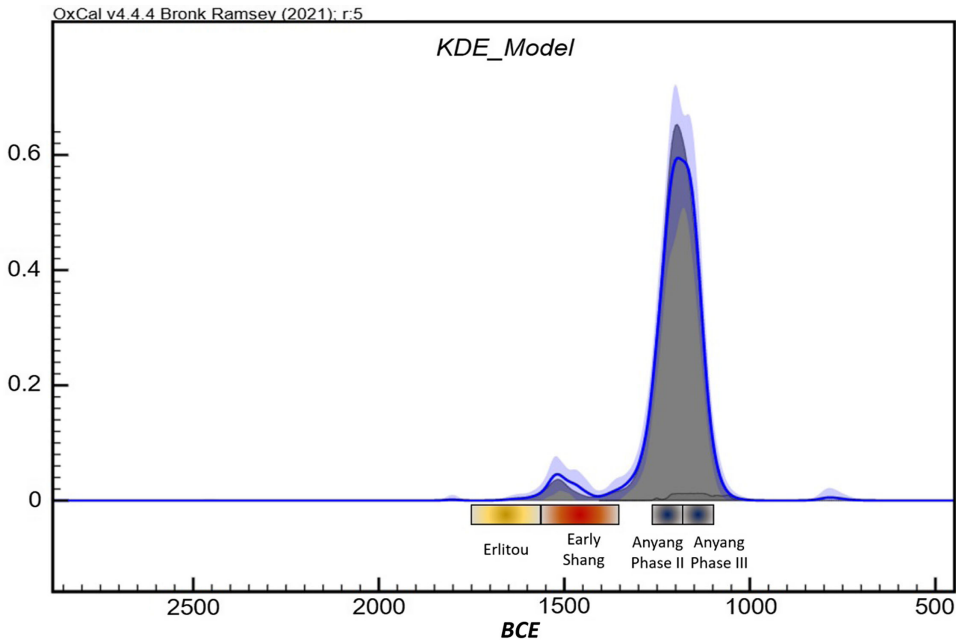


Figure 5 Kernel density estimation of the radiocarbon age for Zaolinhetan with superimposed chronological phases of the Shang Dynasty in the Central Plains.

(XD-18, animal bone) was found in H107, indicating the earliest occupation at Zaolinhetan should be dated to the late Neolithic Longshan period (ca. 2500 BCE). However, the majority of radiocarbon dates fall into the equivalent of the Shang period of the Central Plains (ca. 1500–1046 BCE). As a proxy for human activities (Chaput et al. 2016; Crema 2022), the first peak of radiocarbon dates in the kernel density estimation corresponds well with the transition between the end of the Erlitou period (presumably the last capital of the Xia dynasty) to the rise of the early Shang dynasty, dated to around 1600–1400 BCE. This dating includes different areas of Zaolinhetan, ranging from the house F1 in northwest and trash pit H7 in south (Figure 2). The subsequent phase shows the highest intensity of human activity, which can be undoubtedly dated to 1300–1100 BCE, with over 90% of the radiocarbon dates contributing to a large peak in the kernel density distribution. Its rapid rise and fall is of great archaeological interest as they are roughly consistent with the dates of the late Shang dynasty, as exemplified by its last capital at Anyang. It is also interesting to note that with the exception of seven samples (Beta-1/2/13/17 dated to 1000–800 BC and Beta-14/18-19 to ca. 800–700 BCE, Zaolinhetan was virtually abandoned from the end of the Shang dynasty. In addition to the radiocarbon chronology, the wide dispersion of $\delta^{13}\text{C}$ is also intriguing, which is almost certainly due to the use of C4 plant millet for human diet or animal fodder (Chen et al. 2019; Liu et al. 2021).

Comparison with Traditional Typo-Chronology

The initial brief archaeological excavation report tentatively divides Zaolinhetan into three phases based on the stratigraphy and pottery typology. The first phase is characterized by the coarsely made sand-tempered grey pottery, including *Li*, *Yan*, *Pen*, *Guan* and *Zeng*. The category of *Li* pottery was dominated by the well-known high-necked and stout-legged tripod

(HNSL), which has been the center of the debate on the social identity of the pre-Zhou people for decades (see below). The excavators pointed out that the legs of the majority of HNSL are conical and solid, with their ends being flat, a special feature that allows them to be dated to the Yinxu II phase or later (Table 1), as exemplified by the Duanjing site (Lian 1999; Lei 2010: 83–88; Zhang 1989: Fig. 1, Fig. 6, F3:11, H88 ④:92, H13①a:12). The second phase of Zaolinhetan is marked by a change in HNSL and the increasing proportion of *Li* with jointed crotch. A flat and wide strip of clay was added under the rim of HNSL for decorative purpose and their legs became more separated and conical, with their more pointed tips (Fig. 6, M4:2, H88 ②:8). Similar pottery has also been discovered in the Nianzipo culture and Caijiahe site (Hu 2007: 274–276). All of these have long been assumed to be features of the Yinxu Phase IV (Lei 2010: 147–152). Evidence for the third phase comes from exaction of H103, with more similar chance findings being discovered from the higher position of Zaolinhetan through survey (Figure 6, H103 ③:23). The major groups of pottery are grey and black, decorated by corded or diamond patterns. The legs of *Li* are joined in an arc shape and become smaller, which relates this period directly to the typical Mid-Western Zhou dynasty (Kings Zhao and Mu; Zhang 1999:99–101).

Although the similarities in pottery typology have drawn a few major pre-Zhou and western Zhou sites into comparison with Zaolinhetan (Figure 6), the new radiocarbon data show a significantly narrower chronological span than previously thought (Dou et al. 2019; Li 2020), indicating that these changes took place either at a much faster pace or simultaneously. The issue of applying typological variation to chronological reconstruction is that it is almost impossible to estimate the associated uncertainty of the time elapsed, since pottery typology is essentially tied down to stratigraphic order therefore reflection of relative chronology. This becomes more challenging in the context of a small-scale site since the local material culture could be replaced more easily than that of the large ones. The competing hypothesis is that small sites could be less well-connected and therefore their object styles appear to be more inert and last longer.

In the case of Zaolinhetan, the abundant material remains unequivocally dated to 1300–1100 BCE highlight the fact that the typological changes observed from pottery happened in a very short period of time, implying many typical pottery styles, such as HNSL or jointed crotch *Li*, were in fact co-existent rather than sequential. Moreover, the *Li* vessel (H103③: 23), which is characterized by its flared mouth, curved rim, low and jointed crotch and pointed legs, which for decades has been assumed to be a marker of middle Western Zhou (ca. 9th century BCE), turns out to be associated with the early Yinxu periods (ca. 1200 BCE). This surprisingly early result raises new questions regarding stylistic innovation and, more importantly, to what degree is it legitimate to use pottery style to associate different groups of people and political changes (Hein 2016, 2022; Jaffe et al. 2018). It is likely that the original design of the *Li* vessel as such were derived from the small site of Zaolinhetan but remain absent in archaeological records until middle Western Zhou. Alternatively, this was completely lost after Zaolinhetan and reinvented during the middle Western Zhou. Whilst the link in between is still missing, the new radiocarbon chronology implies that more possible scenarios should be taken into consideration.

Social and Environmental Context of the Collapse of Zaolinhetan

How to correlate the material culture with the specific groups of people such as the pre-Zhou recorded in various textual evidence is a notoriously thorny task in Chinese archaeology. But it is particularly important for the understanding of the state formation and social identity of early dynastic China (Rawson 1999; Liu and Chen 2012; Sun 2015:501–571). A variety of textual evidence demonstrate that the Ji family was the leader of the pre-Zhou people who

Culture	Faoli type	Anyang Phase I	Anyang Phase II	Anyang Phase III	Anyang Phase IV	
Nianziipo Culture	HNSL Li	Nianziipo H151:92 (li) Nianziipo H118:3 (guan)	Caijiabe H31:1 (li)	Caijiabe H21:6 (pen)	Caijiabe H21:7 (pen)	Nianziipo M191:1 (li) Caijiabe H22:10 (pen)
		Nianziipo H1104:30 (guan) Nianziipo H1104:40 (yan)				Caijiabe H22:4 (guan)
Zhengjiapo Culture	Jointed Crotch Li	Andi Y4:14 (guan) Andi H14:11 (pen)	Zhengjiapo H2:8 (li)	Zhengjiapo H2:4 (pen)	Andi H30:7 (li) Zhengjiapo H13:12 (pen)	Beilu Y1:1 (li) Zhengjiapo H19:15 (pen)
		Andi H14:15 (guan)	Andi H7@: 2 (guan)	Zhengjiapo H14:30 (guan)		Zhengjiapo H15:3 (guan)
Sunjia Culture	Divided Crotch Li	Sunjia 2C:3 (li) Sunjia 3A:1 (pen)	Zaoshugounao H212:24 (li)	Zaoshugounao H346:6 (li)	Zaoshugounao H212:8 (pen)	Zaoshugounao H348:5 (li) Zaoshugounao H279:3 (pen)
		Sunjia 2B:5 (guan)	Zaoshugounao H212:26 (yan) Zaoshugounao H353:1 (sanzuweng)	Zaoshugounao H348:8 (guan) Zaoshugounao F14:9 (sanzuweng)		
Duanjing site	Hua Bian Li	Duanjing H17:2 (li) Duanjing G1:19 (dou)	Duanjing M6:1 (li)	Duanjing M7:1 (li)	Duanjing T202@:4 (li)	
		Duanjing G1:20 (guan) Duanjing H22:8 (dou)	Duanjing H8:1 (guan)	Duanjing M7:2 (gui)	Duanjing H2:11 (dou)	
Lijiaya Culture	Hua Bian Li		Lijiaya T46@b:9 (li)	Lijiaya T13H1:1 (li)	Lijiaya T46@a:7 (pen)	Lijiaya T18@a:15 (li) Lijiaya T18@a:47 (guan)
			Lijiaya T46@b:16 (guan)	Lijiaya C2T1@:15 (dou)	Lijiaya T18@a:23 (dou) Lijiaya T18@a:40 (sanzuweng)	
Zaolinhetao Site	HNSL Li		F3:11 (li) H88@:92 (li) H13@a:12 (li)	M4:2 (li)	H8@:8 (li)	M4:3 (guan) H88@:14 (guan)
	Jointed Crotch Li			H103@:23 (li) H103@:46 (pen)		
	Divided Crotch Li			H45@:2 (li) H91:75 (yan)		

Figure 6 Traditional ceramic typological sequence for Zaolinhetao and other key sites.

overthrew the Shang and established the Zhou dynasty. It was also very likely that the army which surrounded the Ji family was a combination of various groups, including their most important ally, the Jiang family. Some scholars argue that the totality of the material culture created by the Ji group should be defined as the pre-Zhou culture (Liu 1991), whilst others tend to take a broader perspective by stating that the material culture of other groups who worked closely with the Ji people should also be considered as part of the pre-Zhou culture, such as the Jiang group (Niu 1998). Bearing in mind the intrinsic fluidity in social identity, one should avoid a static approach which often equates one characteristic type of objects with a specific group of people. It is also likely that the composition of the pre-Zhou people was very diverse and involved many others in different time periods, therefore the term “pre-Zhou” should be considered as a big umbrella rather than a specific identity (Wang 2018).

One of the most important clues for tracing the origin of the pre-Zhou people is from the transmitted text, which states that Gugong Danfu (the great grandfather of the King Wu who conquered the Shang capital Anyang) moved from Bin to Qi. Qi has now been identified as Zhouyuan based on various bronze inscriptions and historical texts, but the exact location of Bin remains unclear. A number of observations point to the Jing River valley as the most likely region for Bin. This has been indicated in several historical transmitted texts, of which the earliest can be traced to the Eastern Han dynasty (25–220 CE), such as the Book of Han and the Book of Later Han. Although it is questionable to what degree these records are accurate with regards to what happened one thousand years ago, several major pre-Zhou sites (e.g., Zaoshugou, Sunjia and Duanjing) provide rich materials that could be related to the pre-Zhou culture. In particular, the most recent discovery of Xitou, which is so far the second largest Zhou site with numerous high-elite burials, adds more weight to the identification of the Jing River being the ancient Bin region.

Both Liu and Zhang (Liu 2003:17–21; Zhang 2004:274–276) contend that jointed crotch *Li* in the Zhengjiapo archaeological type represent the Ji-group (Figure 6, Zhengjiapo Culture), whereas the Jiang group could be identified by HNSL in the Liujia culture (Figure 6, Nianzipo Culture). A completely different opinion proposed by Lei (2010:300–301) is that the change from HNSL to jointed crotch *Li* represents a chronological progression, rather than different groups of people in parallel. Therefore, both types of *Li* pottery should be considered as remains of the (pre-) Zhou people. The new chronology presented here demonstrates that a variety of pottery styles were contemporaneous with one another. This requires a rethinking of the traditional pottery model mentioned above. At least in the case of small-scale sites such as Zaolinhetan, different pottery types, if they could indeed represent different social groups, were actually mixed together in the same place. As a consequence, it is probably not feasible to distinguish different social groups merely based on ceramic typological variation (Jaffe et al. 2018; Liu et al. 2020; Chao 2022).

Moreover, the rapid collapse of Zaolinhetan is also intriguing, which is assigned by the kernel density model to ca. 1100 BCE (Figure 5; Table 2). No evidence is indicative of any rapid environmental deterioration (e.g., flooding), plague, or warfare. The environmental records in the adjacent regions demonstrate relatively stable climate conditions from the Loess Plateau to the Jing River valley, with minor fluctuations in precipitation and temperature (Figure 7) (Zhao 2010; Chen 2015; Zhang 2021:255). The slight decrease in rainfall and colder environment appears unlikely to exert a large impact on agricultural practice, given the introduction of irrigation and local crop diversification, which therefore could mitigate the climate effect. Nevertheless, as indicated by the oracle bone records discovered at Anyang,

Table 2 Summary of key historical events and periods.

Anyang chronological phases	Anyang Phase I	Anyang Phase II	Anyang Phase III		Anyang Phase IV
Late Shang Kings	Pan Geng to Wu Ding (early phae)	Wu Ding (late phase), Zu Geng, Zu Jia	Lin Xin, Kan Ding, Wu Yi, Wen Ding		Di Yi, Di Xin
Xia-Shang-Zhou Chronology Project: archaeological phasing and radiocarbon dating (XSZ Project 2022)	1320–1239 BC	1255–1195 BC	1205–1080 BC		1090–1040 BC
Xia-Shang-Zhou Chronology Project: oracle bones and radiocarbon dating (Five phases) (XSZ Project 2022)	1254–1210 BC	1217–1180 BC	1205–1150 BC	1164–1116 BC	1130–1055 BC
PKU Radioboron Dating Project of Oracle Bones (Five phases) (Liu 2021)	1254–1197 BC	1206–1177 BC	1187–1135 BC	1157–1110 BC	1121–1041 BC
Textual records of key events		King Wuding defeated Gui Fang, Gui Fang surrendered to Yin Shang	The first year of Wu Yi, Gugong Danfu moved to Bin from Qi		
Archaeological cultures along the Jing River		The rise of Sunjia culture	Merge between Sunjia and Nianzipo and southward movement of Lijiaya		Decline in local material culture

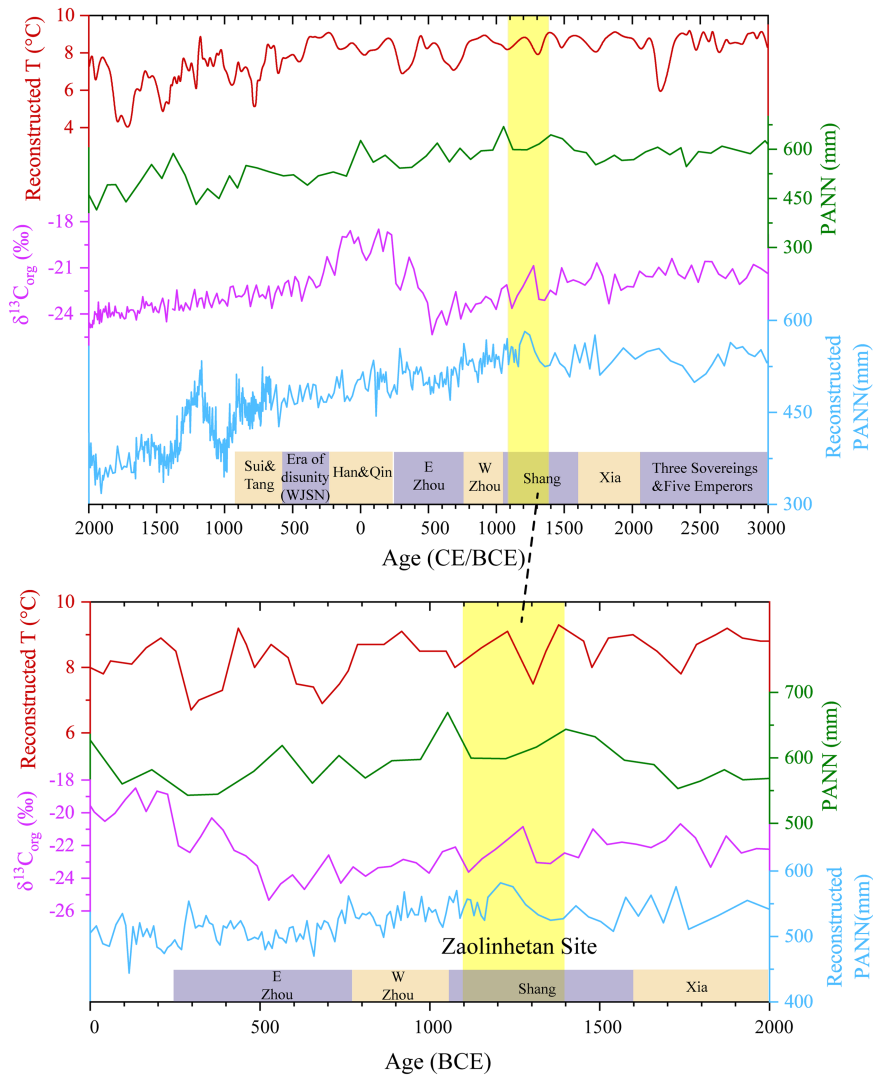


Figure 7 Climate variation for the triangle of Anyang, pre-Zhou and Northerners (the lower figure is the detailed version of the Zaolinhetan period in the upper one; red: branched glycerol dialkyl glycerol tetraethers [Zhang et al. 2021], green, blue lines: pollen data [Zhao et al. 2010; Chen et al. 2015], purple: carbon stable isotopic data of organic carbon [Yang et al. 2023]).

Northern Shaanxi, which is situated on the edge of the summer monsoon and involves both agriculture and animal herding, might have been more affected, resulting in greater social pressure and migration southwards. As recorded in *Bamboo Annals* and *Book of Poetry*, it is due to invasion and harassment by the northern pastoralists (Rong and Di) that caused Gugong Danfu to move from Bin to Qi, which later became the capital of the Zhou dynasty.

In addition to the environmental factors, the other side of the coin is various social factors, which are probably more crucial to understand the abandonment of Zaolinhetan. The broadest picture was the triangular dynamics between Anyang, pre-Zhou people and northerners. Northerners here primarily refer to the people who lived north of the Central Plains and the

Jing-Wei River valley, such as Lijiaya, who relied on a mixed economy of both agriculture and pastoralism. The long-term interaction between Anyang and the northern pastoralists (e.g., Lijiaya, Figure 1), was rooted in the exchange of horses, metal, agricultural products and many other items (Rawson et al. 2020, 2021). Multiple periods of warfare between Shang and the northerners were recorded on the oracle bones (Cao 2021; Li 2018:27–60). However, it is worth noting that very little record of pre-Zhou people can be found on oracle bones at Anyang until the period of Ji Li, the son of Gugong Danfu. Ji Li, who represented the pre-Zhou people at that time, was one vital ally of the Shang in resisting the northerners. During the Anyang Phase II, equivalent to probably the most prosperous time of Zaolinhetan (Figure 5), the Shang King Wu Ding carried out a series of successful military campaigns against the northerners, such as Gui Fang, as recorded in the oracle bones. A peaceful relationship between Shang and northerners lasted until the Anyang Phase III, when the King Wen Ding allied with Ji Li and pushed against the northerners.

The new chronology anchors a precise termination to Zaolinhetan around Yinxu III Phase (Figure 5). This immediately associates its decline to the well-known relocation from Bin to Qi led by Gugong Danfu (Table 1), followed by the rise of such pre-Zhou people as Ji Li in the oracle bone records. Although the archaeological record at Zaolinhetan is essentially limited to pottery remains, lacking any text or inscriptions itself, in the subsequent the Anyang Phase IV, its surrounding sites, however, saw a clear increasing popularity of bronzes and pottery with typical northern stylistic features along the Jing River (Figure 6). The withdraw of pre-Zhou people had left certain degree of vacuum that could be immediately occupied by others. The transformation of local material culture therefore can be also explained by the triangular interaction between the northerners, Anyang and pre-Zhou people.

CONCLUSIONS

A large number of AMS radiocarbon dates derived from well-preserved samples and sound pretreatment, together with the Bayesian modeling that respects the complex stratigraphy, has made the reconstruction of a complete and detailed chronology for Zaolinhetan possible. Its major body of occupation is dated to the 1300–1100 BCE. The rapid decline of Zaolinhetan was presumably a result of the famous event when Gugong Danfu abandoned Bin and moved to Qi. It is very likely that Gugong Danfu moved not only his immediate subordinates but also many others, especially from the surrounding small-scale sites. Not only environmental but also various social factors could contribute to this key migration in early Chinese history. The latter, of which the long-term dynamic triangle between the northern pastoralists, Anyang and the pre-Zhou people, presumably played a larger part. Of course, more radiocarbon work needs to be carried out for the other large- or small-scale sites in this region. If this holds true, then it adds further evidence that Zaolinhetan is in the core area of the ancient Bin region, and its abandonment was directly related to the movement from Bin to Qi by Gugong Danfu.

ACKNOWLEDGMENTS

This work is one of the research outputs funded by Social Science Foundation in Shaanxi China and Innovation Team of Shaanxi Universities (Comprehensive Research of Shang-Zhou Potter at Xitou, Xunyi, Shaanxi. Grant number: 2021G009; The Origin and Early Development of Civilisation on the Loess Plateau). Radiocarbon work at Oxford was supported by ERC advanced project FLAME (670010, Recipient Prof A. Mark Pollard). Dr Ruiliang Liu is also

supported by ERC Synergy Project Horse Power co-funded by ERC (101071707) and UKRI (EP/X042332/1).

SUPPLEMENTARY MATERIAL

To view supplementary material for this article, please visit <https://doi.org/10.1017/RDC.2023.121>

REFERENCES

- Bayliss A. 2009. Rolling out revolution: using radiocarbon dating in archaeology. *Radiocarbon* 51(1):123–147. doi: [10.1017/S0033822200033750](https://doi.org/10.1017/S0033822200033750).
- Blackwell PG, Ramsey CB, Butzin M, Cheng H, Edwards RL, Friedrich M, Grootes PM. 2020. The IntCal20 Northern Hemisphere radiocarbon age calibration curve (0–55 cal kBP). *Radiocarbon* 62(4):725–757.
- Brock F, Higham T, Ditchfield P, Bronk Ramsey C. 2010. Current pretreatment methods for AMS radiocarbon dating at the Oxford Radiocarbon Accelerator Unit (ORAU). *Radiocarbon* 52(3): 103–112.
- Bronk Ramsey C. 1998. Probability and dating. *Radiocarbon* 40(1):461–474.
- Bronk Ramsey C. 2009. Dealing with outliers and offsets in radiocarbon dating. *Radiocarbon* 51(3):1023–1045.
- Bronk Ramsey C. 2017. Methods for summarizing radiocarbon datasets. *Radiocarbon* 59(6): 1809–1833.
- Bronk Ramsey C. 2021. OxCal v4. 4.4. Available at: Retrieved from <https://c14.arch.ox.ac.uk/oxcal.html>
- Bronk Ramsey C, Blaauw M, Kearney R, Staff RA. 2019. The importance of open access to chronological information: the IntChron initiative. *Radiocarbon* 61(5):1121–1131.
- Cao D. 2021. The Loess Highland in a trading network. Beijing: Peking University Press.
- Chao G. 2022. When is a Qin Tomb not a Qin Tomb? Cultural (De) construction in the Middle Han River Valley. *Asian Perspectives* 61(2):253–284.
- Chaput MA, Gajewski K. 2016. Radiocarbon dates as estimates of ancient human population size. *Anthropocene* 15:3–12.
- Chen F, Xu Q, Chen J et al. 2015. East Asian summer monsoon precipitation variability since the last deglaciation. *Scientific Reports* 5(1):1–11.
- Chen S, Fu W, Liu J, Tang L, Zhai L, Zhao Z, Wen R. 2019. Study on the carbonized plant remains from the Zaolinhe Beach site in Xunyi, Shaanxi. *Southern Cultural Relics* 1:103–112.
- Chen X. 2023. Radiocarbon dating and its applications in Chinese archeology: an overview. *Frontiers in Earth Science* 11. doi: [10.3389/FEART.2023.1064717](https://doi.org/10.3389/FEART.2023.1064717)
- Crema ER. 2022. Statistical inference of prehistoric demography from frequency distributions of radiocarbon dates: a review and a guide for the perplexed. *Journal of Archaeological Method and Theory* 29(4):1387–1418.
- Dou H, Wang Z, Zhai L, Zhao Y, Qian Y. 2019. A Brief Report on the Excavation of the Shang and Zhou Period Remains at the Zaolinhe Beach Site in Xunyi County, Shaanxi. *Archaeology* 10:15–32.
- Grundmann JP. 2019. Command and commitment: terms of kingship in Western Zhou bronze inscriptions and in the Book of Documents. Doctor of Philosophy. University of Edinburgh.
- Hein A. 2016. The problem of typology in Chinese archaeology. *Early China* 39:21–52.
- Hein A. 2022. Culture contacts in ancient worlds: a review of theoretical debates and practical applications. *Journal of World History* 33(4): 541–579.
- Hu Q. 2007. Nanbinzhou-Nianzi Slope. Beijing: World Book Publishing Company. p. 274–276.
- Jaffe Y. 2020. Recent research on the Western Zhou period: Introduction to the 2019 essays. *Archaeological Research in Asia* 23:100160.
- Jaffe Y, Wei Q, Zhao Y. 2018. Foodways and the archaeology of colonial contact: rethinking the Western Zhou expansion in Shandong. *American Anthropologist* 120(1):55–71.
- Lei X. 2010. Exploring the Pre-Zhou Culture. Beijing: Science Press.
- Li F. 2010. Bureaucracy and the State in Early China Governing the Western Zhou. Translation by Minna W. Beijing: Sanlian Bookstore.
- Li F. 2018. Compilation and research on oracle bone military inscriptions. Beijing: Zhonghua Book Company. p. 27–60.
- Li Y, Chen T, Liu H, Dou H. 2019. A Study on the Subsistence Economy of the Pre-Zhou Period in Ancient Bing Region Based on the Animal Remains from the Zaolinhe Beach Site in Xunyi, Shaanxi. *Chinese Agricultural History* 4:33–42.
- Li Y, Zhang C, Wang Z, Dou H, Liu H, Hou F, Ma M, Qian Y, Chen H. 2020. Animal use in the late second millennium BCE in northern China: Evidence from Zaoshugou and Zaolinhetan in the Jing River valley. *International Journal of Osteoarchaeology* 30(3):318–329.

- Lian X. 1999. Excavation report of Duanjing Site in Bin County, Shaanxi. *Acta Archaeologica Sinica* 1:73–96.
- Lin Y. 2019. Rectifying the name of typology. Translated by Gu T. *Methodology of prehistoric archaeology by Montelius*. Beijing: Beijing Commercial Press. p. 1–23.
- Liu J. 1991. A Preliminary Understanding of the Connotation of Pre-Zhou Culture. In: *Festschrift Celebrating the 90th Birthday of Mr. Wu Boren*. Xi'an: Sanqin Press. p. 49–56.
- Liu J. 2003. *Studies on Pre-Zhou Culture*. Xi'an: Sanqin Press.
- Liu K, Wu X, Guo Z, Yuan S, Ding X, Fu D, Pan Y. 2020. Radiocarbon dating of oracle bones of late Shang period in ancient China. *Radiocarbon* 63(1):155–175.
- Liu L, Chen X. 2012. *The archaeology of China: from the late Paleolithic to the early Bronze Age*. Cambridge: Cambridge University Press.
- Liu R, Pollard A M, Schulting R, Rawson J, Liu C. 2021. Synthesis of stable isotopic data for human bone collagen: A study of the broad dietary patterns across ancient China. *The Holocene* 31(2):302–312.
- Liu Y, Wang Y, Flad R, Lei X. 2020. Animal sacrifice in burial: materials from China during the Shang and Western Zhou period. *Archaeological Research in Asia* 22(C):100179.
- Niu S. 1998. Exploring the Pre-Zhou Culture. *Cultural Relics Quarterly* 2:40–57.
- Rawson J. 1999. Western Zhou Archaeology. In: Loewe M, Shaughnessy E. *The Cambridge history of ancient China: from the origins of civilization to 221 BC*. Cambridge: Cambridge University Press. doi: [10.1017/CHOL9780521470308.008](https://doi.org/10.1017/CHOL9780521470308.008). p. 352–449.
- Rawson J, Chugunov K, Grebnev Y, Huan L. 2020. Chariotry and prone burials: reassessing late Shang China's relationship with its northern neighbours. *Journal of World Prehistory* 33: 135–168.
- Rawson J, Huan L, Taylor WTT. 2021. Seeking horses: allies, clients and exchanges in the Zhou Period (1045–221 BC). *Journal of World Prehistory* 34(4):489–530.
- Reimer PJ, Austin WEN, Bard E, et al. 2020. The IntCal20 northern hemisphere radiocarbon age calibration curve (0–55 cal kBP). *Radiocarbon* 62(4):725–757. doi: [10.1017/RDC.2020.41](https://doi.org/10.1017/RDC.2020.41)
- Sun Q. 2015. *Tracing the Three Dynasties*. Shanghai: Shanghai Ancient Books Publishing House. p. 501–571.
- Wang L. 2018. Reconsidering the exploration of “Pre-Zhou Culture”. In: *New Fruits Collection (II): Festschrift Celebrating the 80th Birthday of Mr. Lin Yun*. Beijing: Science Press. p. 176–192.
- Xia-Shang-Zhou Chronology Project (XSZ Project). 2022. *Xia-Shang-Zhou Chronology Project*. Beijing: Science Press.
- Yang R, Zhou A, Zhang H, Chen L, Cao K, Huang Y, Lu Y, Dong W. 2023. Mid and late Holocene climate changes recorded by biomarkers in the sediments of Lake Gouchi and their relationship with the cultural evolution of northern Shaanxi. *Progress in Physical Geography: Earth and Environment* 0309–1333. doi: [10.1177/03091333231159007](https://doi.org/10.1177/03091333231159007)
- Yu W. 1996. On the issue of archaeological typology. In: *What is archaeology—selected theoretical papers of Yu Weichao on Archaeology*. Beijing: Chinese Social Sciences Press. p. 54–107.
- Zhang C. 1999. *Zhangjiapo Western Zhou Cemetery*. Beijing: Encyclopedia of China Publishing House. p. 99–101.
- Zhang C, Zhao C, Zhou A, et al. 2021. Quantification of temperature and precipitation changes in northern China during the “5000-year” Chinese history. *Quaternary Science Reviews* 255:106819.
- Zhang T. 1989. A study on the high-collared, pouch-footed Gui. *Cultural Relics* 6:33–43.
- Zhang T. 2004. *Studies on the Shang Culture in the Guanzhong Region*. Beijing: Cultural Relics Press.
- Zhang Z. 1983. Several Issues in stratigraphy and typology. *Cultural Relics* 5:60–69.
- Zhao Y, Chen F, Zhou A, et al. 2010. Vegetation history, climate change and human activities over the last 6200 years on the Liupan Mountains in the southwestern Loess Plateau in central China. *Palaeogeography Palaeoclimatology Palaeoecology* 293(1–2):197–205.